Strojniški vestnik - Journal of Mechanical Engineering 55 (2009)7-8, 472-483
UDC 621.89:621:833
Paper received: 10.04.2009
Paper accepted: 07.08.2009

Uniform Power Transmission Gears

Gorazd Hlebanja* - Jože Hlebanja
University of Ljubljana, Faculty of Mechanical Engineering

A new type of lubricated gears is presented in this paper, referred to as Uniform Power Transmission Gears (UPTG), which have conformal shaped teeth flanks that enable a more uniform transmission of power and motion. The proposed teeth flanks comprise three arcs: an addendum arc, a dedendum arc, with both of these joined by a connecting arc. These UPT gears have been derived from Hawkins' patented Zero Sliding Gears (ZSG) [4].

The name Uniform Power Transmission Gears derives from the fact that these gears operate during power transmission with an almost constant value of friction and a nearly constant value of power transmission. Thus, the power transmission of the UPT gears occurs simultaneously with the double-contact teeth flanks of the driving and driven gears, which means the transmitted power is divided into two parts: the contact pressure in the contacts is lower, and the gear pair conjugates as helical gears. UPT gears can be produced on common gear cutting machines based on a rolling process where teeth shapes are formed by successive enveloping cuts of a cutter. However, the cutter teeth should be manufactured by the UPT rack profile.

A comparison of the UPTGs with involute-type gears is presented. The radii of curvature are investigated in detail and the velocities in the teeth flank contacts were analyzed. Additionally, an investigation of oil-film thickness using the theory of Hamrock and Dowson is discussed. Owing to the decisive influence of heat caused by friction on gears' scuffing resistance, and the heating of the teeth flanks based on Blok's flash-temperature criterion, we have made a careful study and the results are presented. Because the power transmission with UPTGs occurs mostly by rolling, with only a minor amount by sliding, such gears are very suitable for heavy-duty power transmission at relatively slow speed working conditions.

Keywords: zero sliding gears; conformal helical gears; oil-film thickness; flash temperature; uniform power transmission gears

0 INTRODUCTION

In terms of efficiency, for high-speed applications such as the gear drives of gas turbines, which have high contact velocities and thick oil films based on low viscosity oils, there is little likelihood of making significant improvements to the existing involute technology. However, in low-speed industrial applications it is still possible to improve the efficiency and reduce the manufacturing costs. By making the gears conformal we make it possible to have a many-fold increase in the thickness of the oil film [1]. This means that applications such as wind-turbine gearboxes and winch-gear reducers, which rely on heavy oils to provide an adequate oil-film thickness, could use lighter oils to reduce friction while maintaining the same oil-film thickness. The combination of using lighter oils and a tooth form that has a reduced specific sliding would improve the overall gear-mesh efficiency in these applications. Furthermore, the energy savings can be shown to be substantial over the lifetime of the gear drive. Smaller contact pressures and reduced mesh losses also allow for a reduction in the size of gears and the cost of the related oil-cooling system.

Manufacturing costs are also an important consideration. Many applications are using ever-more-expensive gearings. For example, carburized and ground gears, which although they provide a high level of performance are also very costly. The use of conformal gearings, providing the gears are made to be sufficiently conformal, allows hardened gears to be substituted with less-costly materials while staying within the same size envelope.

In 2007, Höhn, et al. [2] reported on redesigned involute gearing and gear-mesh losses reduction by as much as 68%. This provides

*Corr. Author's Address: University of Ljubljana, Faculty of Mechanical Engineering, Aškerčeva 6, 1000 Ljubljana, Slovenia, gorazd.hlebanja@fs.uni-lj.si

conclusive proof that it is possible to design involute gearings with improved efficiency. The basic technique that they employed was to go to a higher pressure angle, use a shorter tooth height and a lower profile contact ratio, and make wider gears with a helical contact that is sufficient to overcome the reduction in the profile contact ratio. Other significant modifications are given in more detail in [2]. Another, alternative approach that can improve efficiency without the need to resort to wider gears is to consider specific types of non-involute gears [3].

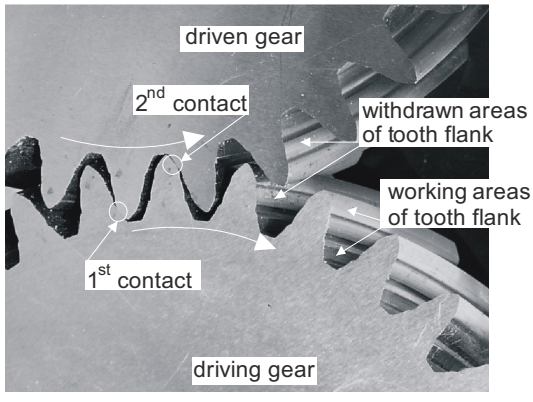

Fig. 1. *Hawkins' zero-sliding gears [9]*

1 HAWKINS' ZERO SLIDING GEARS

Zero sliding gears were granted a US patent in January 2005 [4], and their principle of operation is shown in the photograph in Fig. 1. Hawkins proposed to withdraw a part of the tooth flank relieving central portion of the S gear flanks, thereby eliminating the contacts between teeth flanks in transverse plane of gears. Such gears should be of the helical type so as to enable the transmission of power and the uniform rotation of the driving and the driven gears. During power transmission with these gears, the contact areas of the teeth flanks roll in the axial direction and slide around the pitch point. The addendum and the dedendum of these teeth flanks are shaped by two cycloidal arcs and are separated by the withdrawn parts of the flank. The power transmission from the driving gear to the driven gear occurs over the contact points of the two pairs of teeth, but the first contact is always from the dedendum tooth flank of the driving gear to the addendum tooth flank of the driven gear, with the sliding in the transverse plane and the rolling between the contacting surfaces of the helical lines being in the axial direction. In the second contact the power transmission occurs in the same way, but with reversed relative positions of the teeth flanks. All of the contacts of the gear flanks roll from the front side of the gears to the back side, or vice versa, depending on the direction of the helix. New partners come to contact after every pitch length.

Hawkins describes how these ZSGs, hardened and induction-case-hardened gears, were rig tested without any problems being observed. There was no excessive noise or

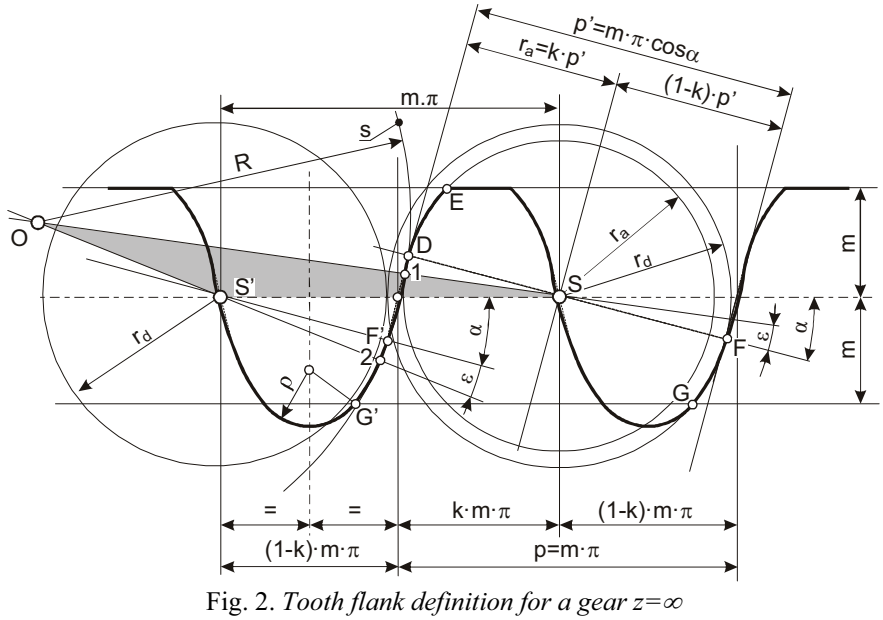

Fig. 2. *Tooth flank definition for a gear z=∞*

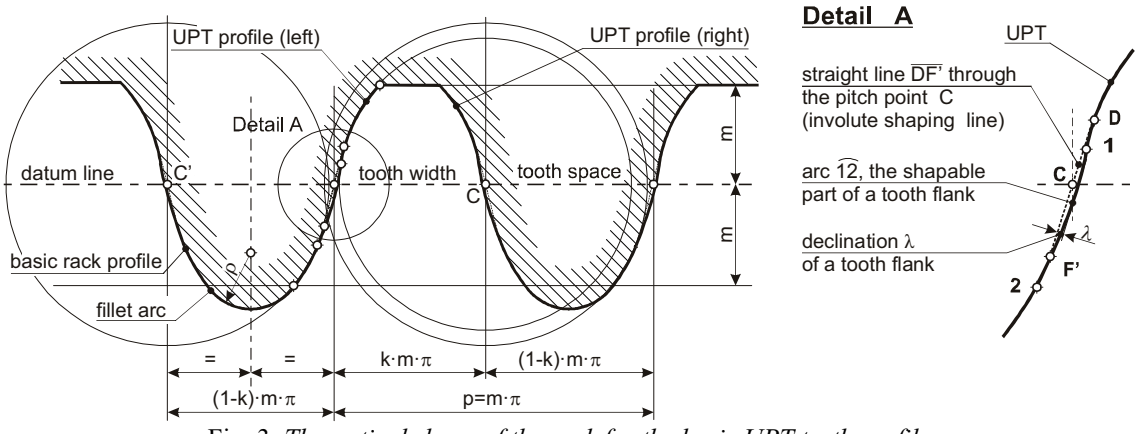

Fig. 3. *Theoretical shape of the rack for the basic UPT teeth profile*

vibration, and no evidence of distress. However, titanium versions of the gears only worked for as long as the coating remained intact; once the coating wore off the gears tended to fail.

2 THE DESIGN OF A NEW RACK PROFILE

The photograph in Fig. 1 shows that the profiles of the ZSG teeth are relatively slim and sharpen to a point. This means that these ZSGs are, more or less, only of theoretical interest and are certainly not suitable for heavy-duty gear applications. It is this observation that led to the idea of developing a new gear type, with the aim to optimize the contact area of the conformal tooth flanks. This new type of gears will be presented and discussed in the paper. We will start with the tooth flank profile for a gear with $z = \infty$, the rack profile, illustrated in Fig. 2. The point S is the centre of the addendum and dedendum circles of the tooth flanks. The line $\overline{DF}$ with the slope angle $\alpha = 15^{o}$ (α could also vary in either direction) is chosen to estimate the radii of these circles. In order to reduce the sensitivity of the gears to deviations in the gears' centre-to-centre distance (from S to S'), radii of the tooth flank profiles for the radius of the addendum r_a and for the radius of the dedendum r_d have been made different. However, the sum of both radii should be kept constant:

$$r_a + r_d = m\pi\cos\alpha = p' . \qquad (1)$$

According to this equation, the addendum radius is $r_a = m\pi k\cos\alpha$, and the dedendum radius $r_d = m\pi(1-k)\cos\alpha$, where the factor $k \le 0.5$, and with which the difference between both radii, $r_d - r_a$, is estimated. The product $m\pi$ is the circular pitch p of the gears, and the product $m\pi\cos\alpha$ is the distance between two neighbouring pairs of teeth contacts. The arc $\widehat{DE}$ from circle r_a, and the arc $\widehat{FG}$ from the circle r_d define the shape of the tooth addendum and the tooth dedendum parts of the teeth flanks of the gears with $z = \infty$. Since the rack cutter is also a gear with the pitch radius $R = \infty$, the teeth flanks are equal, only the tooth spacing and the tooth thickness are changed. Then we shift the arc $\widehat{FG}$ to the left by the length of the circular pitch $p = m\pi$ to the position $\widehat{F'G'}$ and connect both arcs with a new arc $\widehat{12}$, which is part of the circle s with the radius R. In this way the whole tooth profile of the gear with $z = \infty$ or of the rack cutter is defined. If a smooth profile for the tooth flank is required, then point 1 should be placed on the connecting line $\overline{OS}$ and point 2, on the connecting line $\overline{OS'}$. The UPT gears' tooth flank profile of the rack cutter is, therefore, established by the curve E-D-1-2-G'.

With the profile presented in Fig. 3, a new type of rack cutter is used for manufacturing the UPT gears. This is composed of a left- and right-handed tooth profile, connected by fillet arcs with the fillet radius ρ. With such tools the gears can be manufactured with a rolling process, where the teeth formed on the work-piece are shaped by successive enveloping cuts, and the cutting profiles of the rack correspond to this theoretically shaped, basic rack profile.

With regard to an arbitrary gear based power transmission, UPT gears experience backlash, and, therefore, the tooth thickness, s, should be smaller than its space width, e. In our

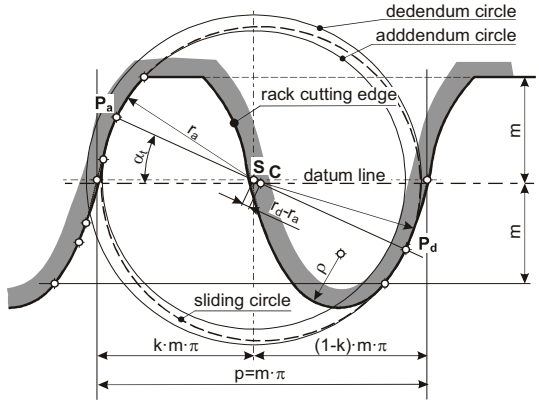

Fig. 4. *UPT rack profile*

case the backlash, *j*, equates to double the difference of the radii $r_d - r_a$, i.e., $j = 2(r_d - r_a)$.

In the transverse plane, the UPT gears are only able to operate with the cylindrical parts of the teeth flanks. This is illustrated in detail A in Fig. 3. The arc $\widehat{12}$ is inserted between the arcs $\widehat{E1}$ and $\widehat{2G}$ (see Fig. 2) of the UPT flank profile, and, therefore, in the region of the rack's datum line the rack-tooth thickness increases by an amount λ on each side. For this reason each successive cut by the enveloping gear tooth becomes increasingly smaller at this point, and, therefore, such gears cannot operate (as observed in the transverse plane) in that part of the tooth flank, but only in dedendum and addendum parts of the gear teeth flanks as helical gears.

The power transmission with UPT gears is shown in Fig.4, i.e., always through the diametrically opposite contacts P_a, for the addendum circle, and P_d, for the dedendum circle, on the tooth flanks. These contact points are situated approximately in the middle of the arcs $\widehat{ED1}$ and $\widehat{F'G'}$ (see Fig. 2), and are located on the connected line P_aSP_d. A circle, named the sliding circle, passes through both contact points, with its centre, C, being equidistant between P_a and P_d. The centre, C, the pitch point, also lies on the datum line (or the pitch line).

The direction $\overrightarrow{P_aCP_d}$ is also the direction of power action. The rack cutter could be designed for the transverse plane, as illustrated in Fig. 4, or for the normal section. In order to apply the same cutting tool a chosen arbitrary module and another helix angle, it would be reasonable to design a cutting tool for the normal section.

3 GENERATION OF UPT GEARS WITH A UPT RACK PROFILE

UPT gears are manufactured by a generating process where the rack-shaped tool (the rack-type cutter, the hob, etc.) with its datum line rolls in the mesh with the gears' pitch circle without sliding, and the rack cutter's teeth flanks form the gear teeth by successive enveloping cuts, as illustrated in Fig. 5. The shape of the cutter's (the hob, the rack cutter, the pinion cutter, the milling head, the grinding tool, etc.) tooth profile should conform to the one defined in Figs. 3 and 4, and to the shape described in Section 3. The main features are the addendum and dedendum circles, which are bound to the datum line of the rack cutter, which means the addendum of the

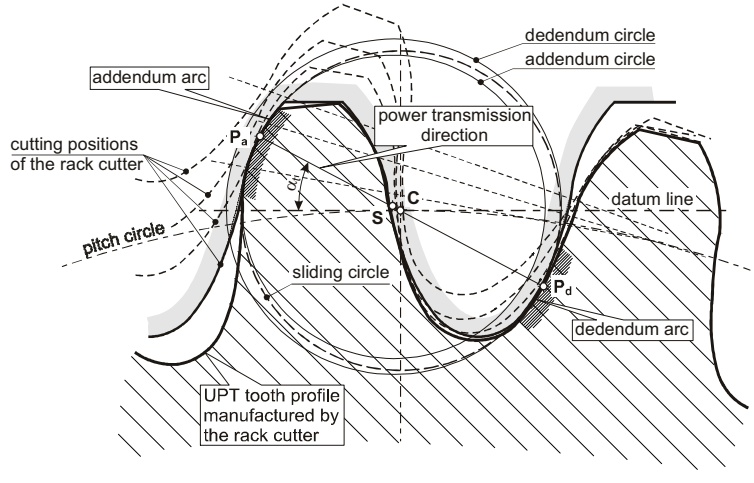

Fig. 5. *Generating UPT gears for any appliance with a UPT profiled cutter*

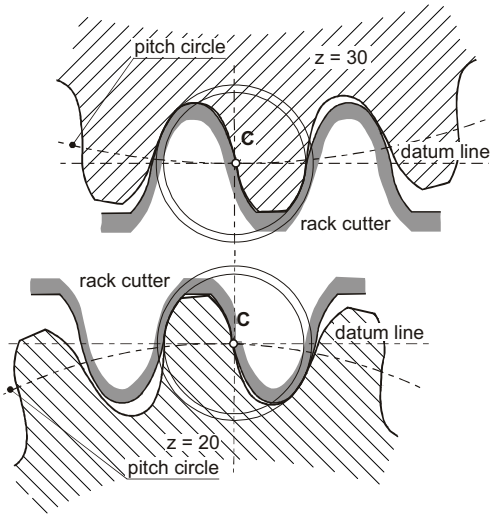

Fig. 6. *Gear teeth generated by the rolling of the rack profile in the mesh over the pitch circle*

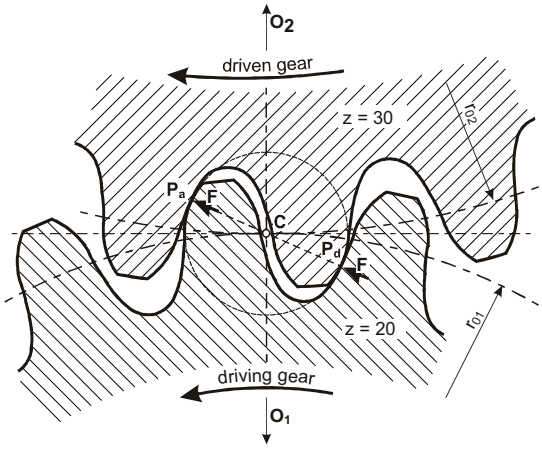

Fig. 7. *Pair of UPT gears with a double concave-convex contact of teeth*

gear tooth becomes the dedendum circle of the rack profile and the dedendum of the gear tooth becomes the addendum circle of the rack profile.

All the gears that are produced with the same shape of rack get teeth with the same radius of addendum r_a, the same radius of dedendum r_d, and the same helix angle β, which implies that all the gears with the same module and the same helix angle β can be manufactured with the single tool. The two gears represented in Fig. 6, i.e., z_1 = 20 and z_2 = 30, are designed with the same rack profile and can work together, as shown in Fig. 7.

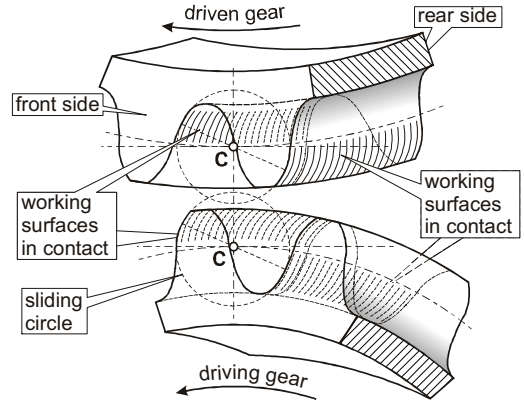

Fig. 8. *Driven and driving UPT gears in axial view*

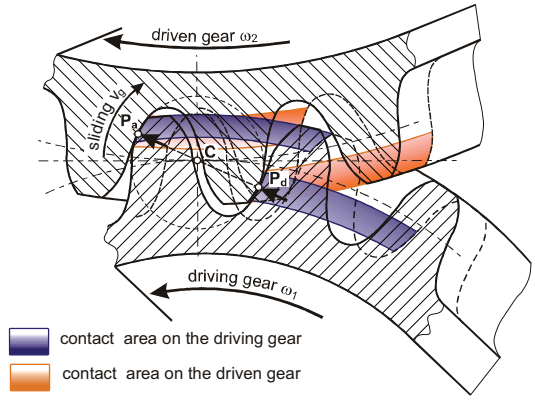

Fig. 9. *UPT gear pair in working position*

There are two concave-convex contacts: the first is at point P_d, where the power transmission between the dedendum of the driving gears and the addendum of the driven gears occurs, and the second, at point P_a, where the transmission from the addendum of the driving gear to the dedendum of the driven gear occurs.

It is important to point out that the gear's teeth are bent in the axial direction, as illustrated in Fig. 8, where the driving and driven gears are presented separately. In the working position both gears should be positioned so that the pitch points C coincide, as schematically shown in Fig. 9. The mutually interacting surfaces are marked and they come into contact at P_a and P_d in the transverse plane, positioned at the pitch point, as exposed in Fig. 9, where the gears are shown in the working position and in the axial view.

4 COMPARISON OF THE INVOLUTE WITH THE UPT TOOTH PROFILE

UPT gears are functional only as helical gears; therefore, they are comparable with helical involute gears. Such a comparison of the tooth shape of involute gears (E-gears) with the tooth shape of UPT gears, in the normal section, is illustrated in Fig. 10 for gears of the same module, the same number of teeth, the same top circle, the same root diameter and the same tooth thickness, s, on the pitch circle. For the tooth profile of the involute gear from Fig. 10a the usable involute tooth profile ends on the base circle. The gears' bending stress depends on the tooth thickness of the dedendum s_f and the height h_f of the load-crossing line with the mid-line of the tooth profile. The corresponding UPT tooth profile is shown in Fig. 10b. The UPT tooth profile is involved in power transmission, both at the addendum and at the dedendum part. It is also evident that the altitude of the load-crossing height is smaller and the tooth thickness of the dedendum s_f is greater to some extent. Fig. 10c illustrates a superposition of both profiles. In comparison to the UPT teeth, the involute teeth are thicker in the pitch circle area and weakened at the bottom area. In terms of the bending strength, the UPT gears are stronger of the two.

5 THE TRANSMISSION OF POWER AND MOTION WITH UPT GEARS

The power transmission between a UPT driving gear and a UPT driven gear is illustrated in Figs. 9, 11 and 12. An important feature of the UPT gears, which can only operate as helical gears, is that they do not possess the normal path of contact in the transverse plane, as depicted in Fig. 11. This figure shows that the teeth flanks move from the working position at A, pass the pitch point C, to the working position B, without any contact between the flanks, and consequently, also without any friction.

From Fig. 12 it can be concluded that the power can only be transmitted over the contacts of the simultaneously loaded surfaces at P_a and at P_d. Both contact spots converge to points on two pairs of helices, one on the pinion and the other on the gear in each pair. The contacts P_a and P_d also represent tangential points of the pinion and the gear helices. From the transverse view in Fig. 12 the rotation and the power transmission from the pinion to the gear with the sliding of the pinion flank surfaces along the gear flanks can be recognised. At the contact point P_d the pinion's dedendum flank slides along the gear's addendum, and at point P_a the pinion's addendum flank slides in the opposite direction across the gear's dedendum flank with velocity v_g. The pinion's helices through points P_a and P_d rotate with the pinion and the gear's helices in the same contact points rotate with the gear. Therefore, also the contact points, that is P_a and P_d are moving in the axial direction by rolling the pinions' helices over the gears' helices in the direction from the pinion and gear front side to their back side.

5.1 The Velocities of the Teeth Flank Contacts

As mentioned above, the same teeth flanks that were in contact at point P_d, came by rotation of the pinion around its axis O_1 and the rotation of the gear around the axis O_2 to the contact at point P_a, which means that the rotation of the pinion and the gear pitch circles for an arc size of one pitch p, and at the same time the contact points P_d and P_a shift from the front side to the back side of the pinion (or gear) for the length of the face

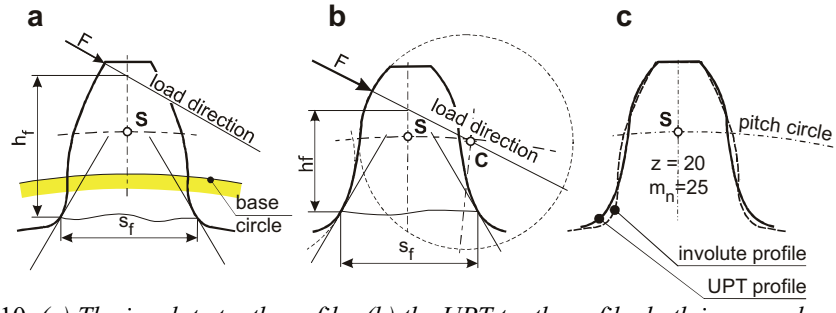

Fig. 10. *(a) The involute tooth profile; (b) the UPT tooth profile, both in normal section; (c) comparison of the involute and UPT shapes*

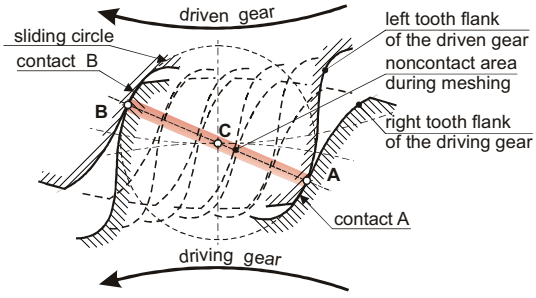

Fig. 11. *Progress of the teeth flanks without contact in the transverse plane from the contact point A to the contact point B during power transmission*

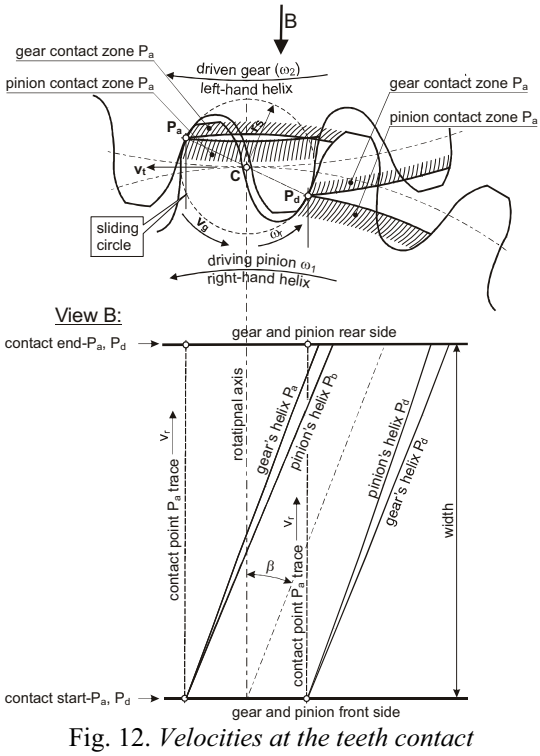

Fig. 12. *Velocities at the teeth contact for the UPT gears*

width b with the rolling velocity v_r. If the pinion rotates with a constant angular speed ω_1, then the gear rotates with a constant angular speed ω_2, and then the pitch line velocity v_t for both the pinion with the pinion pitch radius r_{01} and for the gears with the pitch radius r_{02}, equals:

$$v_t = \omega_1 r_{01} = \omega_2 r_{02}. \quad (2)$$

If the angular velocities ω_1 and ω_2 remain constant over time, then the pitch line velocity v_t will also remain constant for the same interval. At the same time, as the pitch circle passes the length

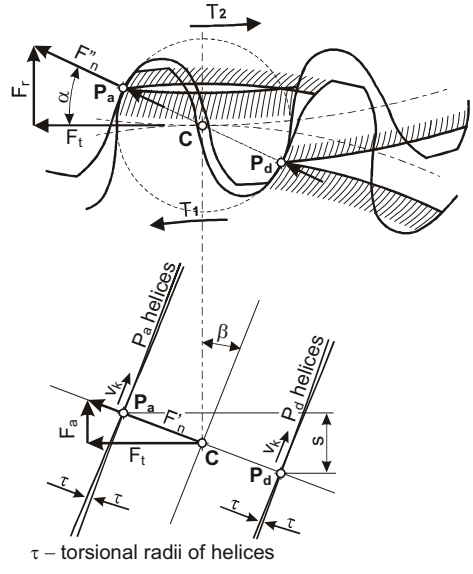

Fig. 13. *Load transmission in the UPT gears*

of the transverse pitch p, the contact points P_a and P_d should be shifted by the face width b, where $b = p/\tan\beta$, (β is the helix angle). From this relation derives the axial velocity of the contact points P_a and P_d in the axial direction from the front side to the back side, v_r:

$$v_r = v_t/\tan\beta. \quad (3)$$

The relative angular velocity ω_r of the pinion and gear around the pitch point is defined as

$$\omega_r = \omega_1 + \omega_2. \quad (4)$$

The sliding velocity, with $r_s = 0.5\ (m\ \pi \cos\alpha)$, between the teeth flanks v_g is

$$v_g = r_s(\omega_1 + \omega_2) = r_s\omega_r. \quad (5)$$

Thus, the angular velocity ω_r and the sliding velocity v_g are proportional. It is important to point out that in case of constant angular velocity ω_r also the sliding velocity v_g remains constant.

5.2 Power Transmission Between the Teeth Flanks

The power transmission for all the gears starts with the driving shaft and the input torque, T_{1in}, which transmits the rotation over the gear teeth with the tangential force F_t to the driven, output shaft with torque T_{2out}. In this way the power is also transmitted with UPT gears, for which a tangential force F_t, a radial force F_r and an axial force F_a with its resultant F_n as a normal

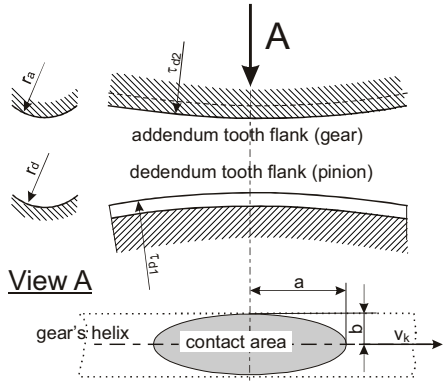

Fig. 14. *Shape of the contact area P_d*

force are presented in Fig.13. From the known input torque T_1 it is possible to derive the tangential force (providing the losses are neglected):

$$F_t = T_1/r_{01}. \tag{6}$$

The normal force F_n acts perpendicularly to the teeth flanks and creates an axial component F_a and a radial component F_r. Therefore, the axial component F_a operates along the gear axis, $F_a = F_t.\tan\beta$, while the radial component F_r operates perpendicularly to the axis $F_r = F_t.\tan\alpha$. In this way the normal force F_n, the force with which the teeth flanks are pressed against each other, is obtained by taking the square root of the sum of the square of all its components:

$$\begin{aligned} F_n &= (F_t^2 + F_a^2 + F_r^2)^{0.5} \\ &= 0.5\, F_n(1 + \tan\beta^2 + \tan\alpha^2)^{0.5}. \end{aligned} \tag{7}$$

Fig. 13 shows that the normal force F_n operates through both contact points P_a and P_d as it does through the pitch point C. Therefore, the contact points P_a and P_d under working conditions in the axial direction fall behind each other for a certain distance:

$$s = m\pi \cos\alpha \sin\beta \tag{8}$$

The input torque T_1 usually remains constant for some time, which is consequently also true for the normal force F_n. This then implies that the power transmission with UPT gears also stays constant during this time period. It is for this reason that these gears have been named Uniform Power Transmission gears, or UPT gears, in short.

5.3 The Shape of the Contacts of the Teeth Flanks

The contacts over which the power transmission occurs are composed of the driving part and the driven part where the driving part presses the driven part over the contact area, resulting in a sliding or rolling motion. The contact areas of the UPT gears are ellipsoidal in shape; this is illustrated by the contact point P_d shown in Fig. 14. The driving pinion with its dedendum part of the tooth, drives the addendum part of the gear tooth, the contact area then rolls along the gear's helix with the velocity v_k, but simultaneously the dedendum flank slides over the addendum flank with the velocity v_g. The axis of the elliptically shaped contact can be defined by the radii of curvature of the helices τ_{d1} and τ_{d2}, as well as by the radii of the tooth flanks r_a and r_d, as shown in Fig. 4 for the contact point P_d.

The tooth flank addendum radius r_a and the dedendum radius r_d are equal for both contact points P_a and P_d. However, the torsional radii of the helices τ_{d1} and τ_{d1} differ in these contact points. The helices are located on the cylinder surfaces with the radius r_{P1} for the pinion and r_{P2} for the gear at the contact point P_d. The torsional radii of helices can be calculated with the formula [8], [10]

$$\tau = (a_r^2 + b_r^2)/b, \tag{9}$$

where a_r equals the radius of the cylinder surface r_P and $b_r = r_P \tan\beta$. Taking into account Eq. (9), the torsional radii of the helices with the course through the contact point P_d are:

$$\begin{aligned} \tau_{d1} &= \frac{r_{P1}^2 + (r_{P1}\tan\beta)^2}{r_{P1}\tan\beta}, \text{ and} \\ \tau_{d2} &= \frac{r_{P2}^2 + (r_{P2}\tan\beta)^2}{r_{P2}\tan\beta}. \end{aligned} \tag{10}$$

The reduced radius of curvature for the rolling contact point P_d is defined by:

$$\frac{1}{\rho_{red,k}} = \frac{1}{r_a} - \frac{1}{r_d} + \frac{1}{\tau_{d1}} + \frac{1}{\tau_{d2}}, \tag{11}$$

whereas the value for the reduced radius of curvature for the sliding contact is:

$$\frac{1}{\rho_{red,s}} = \frac{1}{r_a} - \frac{1}{r_d}. \tag{12}$$

Based on the above explanation, a concave–convex type of contact should exist between the teeth flanks and a convex-convex

type of contact between the helices. In order to illustrate the contact circumstances, some data for gears in Figs. 6 and 7, with m = 25 mm, are presented, such as radii r_a = 37.5 mm, r_d = 41.23 mm, τ_{d1} = 472 mm, and τ_{d2} = 783 mm. The reduced radius for the contact point P_d is thus $\rho_{red,k}$ = 168 mm. A similar result for the reduced radius of curvature can also be expected for the contact point P_a, where the power transmission occurs from the addendum flank of the pinion to the dedendum flank of the gear.

To compare the reduced radii of curvature of the UPT gears to the involute gears, a reduced radius for the involute gear pair of the same size (z_1 = 20, z_2 = 30, m = 25 mm) was calculated, and $\rho_{red,inv}$ = 50.8 mm has been obtained as the maximum value.

5.4 Hertzian Contact Stress

The most commonly used criterion for the pitting durability on gear-tooth flanks is the Hertzian contact pressure. For involute gears a rectangular contact area, $A = 2b\,l$, has to be taken into account, where b stands for half the contact width, l is face width, and the maximum pressure is determined with the following formula [6]:

$$\sigma_H = \sqrt{\frac{F_n}{2\pi l}\frac{E_{red}}{\rho_{red}}} = \sqrt{\frac{w}{2\pi}\frac{E_{red}}{\rho_{red}}} \le \sigma_{\lim}\,. \qquad (13)$$

For a given tangential load F_t for involute gears, the contact load is $F_n = F_t/\cos\alpha$, where $\alpha = 20^o$ and $F_n = 1.064\,F_t$.

For good operating conditions the Hertzian pressure is limited by the allowable pressure σ_{lim}, as well as the reduced radius of curvature ρ_{red} and the specific load $w = F_n/l$, which also have a strong influence on the pressure.

According to Fig.14, an elliptical contact area exists for the UPT gears where the contact pressure can be expressed by the formula [7]:

$$\sigma_H = \frac{F_n}{2ab}\,, \qquad (14)$$

where the expressions for a and b are:

$$a = k_1\left(\frac{3F_n\,\rho_{red}}{E_{red}}\right)^{1/3}\text{, and}$$
$$b = k_2\left(\frac{3F_n\,\rho_{red}}{E_{red}}\right)^{1/3} \qquad (15)$$

from which the following formula is obtained:

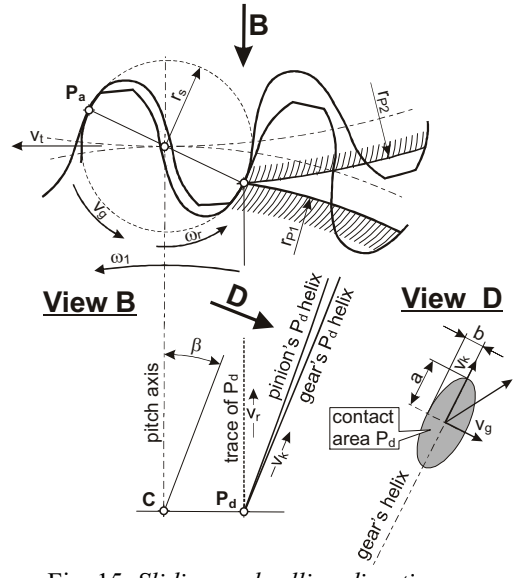

Fig. 15. *Sliding and rolling directions of the P_d contact area*

$$\sigma_H = \frac{3}{2\pi k_1 k_2}\sqrt[3]{\frac{F_n^2\,E_{red}}{3\rho_{red}}} \le \sigma_{\lim}. \qquad (16)$$

For the gears presented in Figs. 6 and 7 following values apply: $k_1 \approx 1.8$; $k_2 \approx 0.63$; ρ_{red} = 168 mm and $F_n = 0.5F_t\,(1+\tan^2\beta+\tan^2\alpha)^{0.5}$, and so for $\alpha = 20°$, $\beta = 25°$ we obtain $F_n = 0.581F_t$. Knowing these data and having in mind the fact that $\rho_{red,inv}$=50.8 mm, it becomes evident that the UPT gears are favourable for power transmission without pitting than the involute gears.

5.5 Lubrication Conditions

The elastohydrodynamic lubrication of UPT gears can be evaluated using the Dowson-Hamrock formula [5]:

$$\frac{h}{\rho_{red}} = \frac{2.69\left(\frac{v_\Sigma\eta_0}{E\rho_{red}}\right)^{0.67}(\alpha E)^{0.53}\left(1-0.61e^{-0.73k}\right)}{\left(\frac{F_n}{E\rho_{red}^2}\right)^{0.067}}, \qquad (17)$$

where h is the oil-film thickness, ρ_{red} is the reduced radius of curvature, v_Σ is the sum of the entering surface velocities, E is the reduced modulus of elasticity for the chosen material, α is the pressure-viscosity coefficient, F_n is the contact load, and k is the ellipticity parameter.

The factors in the oil-film thickness Eq. (17), which are influenced by the gearing itself,

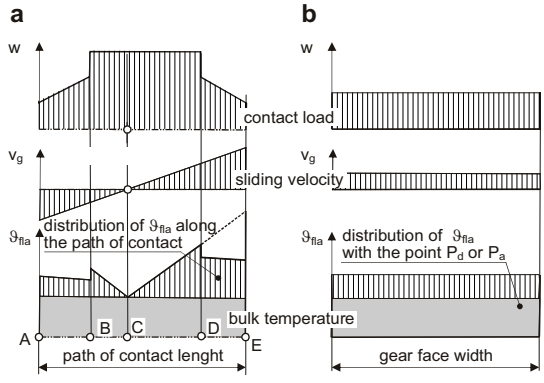

Fig. 16. *Comparison of the contact load, the sliding velocities and the flash temperature (a) of the involute gears [6] and (b) the UPT gears*

are the kinematic factor – the summary velocity, v_Σ, and the geometric factor – the reduced radius, ρ_{red}. In order to estimate the influence of these two factors in a simple way, the Eq. (17) should be reorganised as follows:

$$h = \frac{2.69\left(1-0.61e^{-0.73k}\right)\alpha^{0.53}\eta_0^{0.67}}{E^{0.073}F_N^{0.067}} v_\Sigma^{0.67}\rho_{red}^{0.464}. \quad (18)$$

View D in Fig. 15 shows the elliptical contact area of the teeth contact at position P_d and its direction of movement. In that area the gear tooth surface and pinion tooth surface have the same rolling velocity, v_k, and, perpendicular to that, the sliding velocity, v_g. Based on this the summary velocity, v_Σ, can be obtained:

$$v_\Sigma = \sqrt{v_g^2 + \left(\frac{2v_\kappa}{2}\right)^2} = \sqrt{v_g^2 + v_\kappa^2}\ . \quad (19)$$

From Fig. 15 it is also clear that the rolling velocity should be:

$$v_k = v_r/\cos\beta = v_t/(\tan\beta\cos\beta). \quad (20)$$

Thus, rewriting Eq. (5) gives

$$\omega_1+\omega_2 = v_t(1/r_{01}+1/r_{02}), \quad (21)$$

and for $r_g = 0.5m\pi\cos\alpha_P$ the sliding velocity comes to:

$$v_g = v_t\frac{z_1+z_2}{z_1 z_2}\pi\cos\alpha_P\,. \quad (22)$$

With the data for the gear pair presented in Figs. 6 and 7 and values for $\alpha_P = 20^o$ and $\beta = 25^o$ the resulting velocities gain the following values: $v_k = 2.366v_t$, $v_g = 0.246v_t$, and $v_\Sigma = 2.379v_t$.
The sliding velocity, v_g, only contributes about ~10% to the summary velocity, v_Σ, while the rolling velocity is ~90%, which means that the power transmission with UPT gears occurs mainly as a result of rolling between the teeth flanks. The values of the sliding and the rolling velocities remain proportional to the tangential velocity v_t during the whole period of the gear's operation. In this particular case with regard to Eq. (18), the summary velocity contributes to the oil-film thickness with a factor $(2.379v_t)^{0.67}$ and the reduced radius of curvature $\rho_{red,k}$=0.168 m, with the factor $0.168^{0.464}$=0.437. For involute gears of the same size and characteristics a smaller reduced radius of curvature, ρ_{red}, is characteristic and consequently the lubrication conditions with respect to involute gears are worse than with UPT gears.

5.6 Endurance with Regard to Scuffing and Wear

Scuffing is a severe form of gear-tooth surface damage in which seizure of the tooth surface occurs. This is due to the absence of a lubricant between the contacting teeth flanks of the mating gears. The risk of scuffing damage varies, depending on the sliding velocity, the load, the gear materials, the lubricant used, the surface roughness, etc. The high surface temperatures due to high surface pressures and sliding velocities can initiate the breakdown of the lubricant film. Based on this, two approaches to relating the temperature to the breakdown of the lubricant film were proposed, namely a) the flash-temperature criterion based on contact temperatures along the path of contact and b) the integral-temperature criterion. The aim in this paper is to compare the UPT gears to involute gears, according to the resistance of the gear-tooth flanks to scuffing on the basis of the flash-temperature criterion, based on the original Blok's formula [11], [12]:

$$\vartheta_{fla} = 0.62\mu\left(\frac{F_n}{2l}\right)^{0.75}\left(\frac{E}{\rho_{red}}\right)^{0.25}\frac{\left|v_g\right|}{2\sqrt{B_m\Sigma v}} \quad (23)$$

where ϑ_{fla} is the flash temperature caused by friction, μ is the coefficient of friction, F_n is the contact load, E is the reduced elasticity modulus of the gear material, ρ_{red} is the reduced radius of curvature in the contact area, Σv is the summary velocity of the teeth flank surfaces of the pinion and gear in the contact point. In this case the

Fig. 17. *A pair of the UPT gears; m_n=5 mm; z_1=12, z_2=20*

velocities for both flanks are equal, and B_{m1} and B_{m2} are values for the thermal conductivities of both contact flanks (the characteristics of the materials). The product $B_m \Sigma v$ relates to the heat transfer from the surface into the bulk material; a greater velocity implies a lower flash temperature.

Factors in Blok's equation having a decisive influence on the generation of temperature on the gear-teeth surfaces are the friction coefficient μ, the contact load w, the reduced radius of curvature ρ_{red} and the sliding velocity v_g.

In order to evaluate the effect of friction on the flash temperature the following frequently cited expression [6] has been employed:

$$\mu = 0.045\left(\frac{w}{v_\Sigma \rho_{red}}\right)^{0.2} \eta_M{}^{-0.05} \mathrm{X}_R, \qquad (24)$$

where $w = F_N/l$, η_M is the oil viscosity and X_R is the coefficient of the surface roughness. The summary velocity $v_{\Sigma,inv} = v_{r1}+v_{r2}$ for the involute gears varies and depends on the distance of the contact point along the path of contact from the pitch point. However, for the UPT gears the summary velocity $v_{\Sigma,\mathrm{UPT}} = r_s(\omega_1+\omega_2)$ remains constant over time.

For UPT gears the contact load of the tooth flanks, w, is divided between two pairs of contacts for gear-tooth flanks and remains constant.

The reduced radius of curvature ρ_{red} for the involute gears is formed by two cylinders (the contact area is rectangular) and for the UPT gears it is formed by two pairs of contacts (the ellipsoidal contact area). The reduced radius of the UPT gears appears to be greater than that of the involute gears.

It was also stated that the summary velocity v_Σ for the UPT gears is, because of the axial motion of the contacts, much higher than for the involute ones. The sliding velocities of the involute gears are at the extreme points of contact A and E (the path of contact limits) greater than v_g for the UPT gears.

All the discussed factors have a big influence on the technical characteristics of the gears. The corresponding differences between UPT and involute gear factors are summarised in Fig. 16.

6 UPT GEAR PAIR MODEL

Using the data presented in Section 2, a gear cutter was produced and some gear pairs were shaped afterwards with a Maag shaping machine. A gear pair produced in this way is presented in Fig. 17. These gears were designed with the purpose of geometry and kinematics evaluation. Since it was necessary to lower the costs they were produced from commercially available aluminium. By employing a simple apparatus it has been demonstrated that the power transmission of UPT gears is in agreement with the presented theory. Furthermore, it has also been proven that such gears could have been produced by any of the common methods for gear manufacturing using the appropriate cutting tools.

7 CONCLUSIONS

Many fields of application exist where it is necessary to use lubricated gears for power transmission, and where diminishing the power losses and mechanical noise appear to be of crucial importance [13]. Both prevailingly depend on the form of the teeth flanks [14]. Therefore, the research work has focused on finding solutions to this problem. The proposed UPT gears have been developed as a research effort in this direction.

The essential element of the UPT gears is the absence of a pitch line and the gear-teeth contact in the transverse plane. In addition, there is no sliding between the teeth flanks in the transverse plane. From Figs. 13 and 14 it can be observed that power is mainly transmitted by the

rolling of the teeth flanks at the contact points P_a and P_d, with the simultaneous sliding of the teeth flanks around the pitch point C. The contact load is divided into two contact points. Better lubrication conditions can be expected as a result of the thicker oil-film thickness as it follows from Eq. (18). Due to the characteristics of the UPT gears a lower flash temperature can be anticipated, as it can be derived from Eq. (23). However, the most important features of the UPT gears are constant sliding, constant power transmission and reduced heat generation. The above mentioned features indicate that UPT gears can be used with heavy loads in non-stop operating condition, for example, in the power transmission of wind turbines, gear units for refinery services, and similar applications.

8 REFERENCES

[1] Hlebanja, J. Influence of the Path of Contact Shape and Sliding Condition between Tooth Flanks. *JSME International Conference on Motion and Power Transmission*, Hiroshima, *MPT'91, 1D1*, 1991. p. 560-564.

[2] Höhn, B.R. Improvements on Noise Reduction and Efficiency of Gears. *ECOTRIB 2007.* Slovenian Society for Tribology, Ljubljana, 2007. p. 829-845.

[3] Hlebanja, G., Hlebanja, J., Okorn, I. Research of Gears with Progressive Path of Contact. *Proceedings of DETC'00; Int. Power Transmission and Gearing Conf.,* Sept. 10-13, 2000, Baltimore. DETC2000/ PTG-14384, p. 1-7.

[4] Hawkins, R. Non-involute Gears with Conformal Contact. *US patent 6,837,123.* United States Patent and Trademark Office, Alexandria. 2005.

[5] Dowson, D., Higginson, G.R. *Elasto-Hydrodynamic Lubrication. SI Edition.* Pergamon Press, Oxford, 1977. p. 96. ISBN 0-08-021303-0.

[6] Nieman G., Winter H. *Machine elements, Vol. II: General topics about Gearings, Basics, Cylindrical Gears.* Springer Verlag, Berlin, Heidelberg, New York, 1989. p. 140, 158, 223,. ISBN 3-540-11149-2.

[7] Stachowiak, G.W., Batchelor, A.W. *Engineering Tribology.* 2nd ed. Butterworth Heinemann, 2001. p. 356. ISBN 0-750-67304-4.

[8] Bronstein, I.N., Semendjajev, K.A., Musiol, G., Mühlig, H. *Pocket-book of mathematics.* TZS, Ljubljana, 1997. p. 211-212, ISBN 86-365-0216-0

[9] Hawkins, R. A manufactured ZSG gear pair. 2005.

[10] Kreyszig, E. (2006) *Advanced Engineering Mathematics.* 9th Ed. Willey International. p. 397. ISBN 978-0-471-72897-9.

[11] These, F.H. Blok's Flash Temperature Hypotesis and its Practical Application in Gears. *Schmiertechnik* 14 (1967), Heft 1, p. 22-29.

[12] Blok, H. The Flash Temperature Concept. *Wear*, vol. 6, 1963. p. 483-494.

[13] Belšak, A., Flašker, J. Vibration Analysis to Determine the Condition of Gear Units. *Strojniški vestnik – Journal of Mechanical Engineering,* Januar 2008, vol. 54, no.1, p. 11-24.

[14] Hlebanja, G., Hlebanja, J., Čarman, M. Cylindrical wormgearings with progressively curved shape of teeth flanks. *Strojniški vestnik – Journal of Mechanical Engineering,* Januar 2009, vol. 55, no.1, p. 5-14.